

Use of Carbonaceous Polysaccharide Microspheres as Templates for Fabricating Metal Oxide Hollow Spheres

Xiaoming Sun,^[a, b] Junfeng Liu,^[a, b] and Yadong Li*^[a, b]

Abstract: A general method for the synthesis of metal oxide hollow spheres has been developed by using carbonaceous polysaccharide microspheres prepared from saccharide solution as templates. Hollow spheres of a series of metal oxides (SnO₂, Al₂O₃, Ga₂O₃, CoO, NiO, Mn₃O₄, Cr₂O₃, La₂O₃, Y₂O₃, Lu₂O₃, CeO₂, TiO₂, and ZrO₂) have been prepared in this way. The method involves the initial absorption of metal ions from solution into the functional surface layer of carbonaceous saccharide microspheres; these are then densified and cross-linked in a subsequent

calcination and oxidation procedure to form metal oxide hollow spheres. Metal salts are used as starting materials, which widens the accessible field of metal oxide hollow spheres. The carbonaceous colloids used as templates have integral and uniform surface functional layers, which makes surface modification unnecessary and ensures homogeneity of the shell. Macroporous

films or cheese-like nanostructures of oxides can also be prepared by slightly modified procedures. XRD, TEM, HRTEM, and SAED have been used to characterize the structures. In a preliminary study on the gas sensitivity of SnO₂ hollow spheres, considerably reduced "recovery times" were noted, exemplifying the distinct properties imparted by the hollow structure. These hollow or porous nanostructures have the potential for diverse applications, such as in gas sensitivity or catalysis, or as advanced ceramic materials.

Keywords: hollow spheres • metal oxides • nanostructures • recovery time • sensors • template synthesis

Introduction

The preparation of hollow inorganic capsules of defined structure and composition, with tailored properties, is of immense scientific and technological interest. These hollow nanostructures have either found, or are proposed to have, diverse and fascinating applications, such as in the encapsulation and controlled release of various substances (e.g., drugs, dyes), catalysis, acoustic insulation, waste removal, combinatorial synthesis, the formation of photonic bandgap crystals (PBG), the development of piezoelectric transducers and low dielectric constant materials, and in the processing of other functional materials.^[1–3]

A variety of chemical and physicochemical procedures have been employed for the manufacture of oxide hollow capsules to take advantage of the diverse functions of oxides combined with the enhanced properties endowed by the hollow structures. These methods include the lost-wax method,^[4] spray pyrolysis,^[5] emulsion/phase separation procedures,^[6] the bubble-template method,^[7] the kinetically controlled template-free synthesis method,^[8–10] and sacrificial-core techniques.^[2,3,11–19]

During the past five years, the synthesis of oxide hollow spheres through sacrificial core techniques has developed considerably. Colloidal nanoparticles (e.g., Au, Ag, or CdS) have been used as templates.^[11–14] Very recently, submicrometer polystyrene spheres have been demonstrated to be powerful templates for many kinds of oxide hollow spheres. They are incorporated into composite core-shell structures, and these are then converted into hollow capsules by thermal or chemical means.^[2,3,15–19] Xia and co-workers have reported the synthesis of TiO₂ and SnO₂ hollow spheres by templating their sol-gel precursor solutions on arrays of crystalline polystyrene particles confined between two substrates.^[15] Caruso and co-workers have reported a layer-by-layer method, whereby they fabricated oxides or hybrid hollow spheres by consecutively assembling small oxide

[a] Dr. X. Sun, J. Liu, Prof. Y. Li
Department of Chemistry, Tsinghua University
Beijing, 100084 (P. R. China)
Fax: (+86)10-6278-8765
E-mail: ydli@tsinghua.edu.cn

[b] Dr. X. Sun, J. Liu, Prof. Y. Li
National Center for Nanoscience and Nanotechnology
Beijing, 100084 (P. R. China)

Supporting information for this article is available on the WWW under <http://www.chemeurj.org/> or from the author.

nanoparticles (<10 nm) and polyelectrolytes onto large polystyrene colloids (submicrometer range) and subsequently removing the templates by calcination or dissolution.^[16] Very recently, Yang and co-workers further developed the template method, and controlled shell thickness and cavity size by templating core-gel-shell particles.^[17]

In spite of these successes, there still exist some challenges for materials scientists to overcome. For instance, most oxide hollow spheres prepared by means of the template method have been centered on a few particular compositions such as SiO₂, TiO₂, SnO₂, ZrO₂, and Fe₃O₄.^[2,3,11–19] Some important oxide functional materials with distinctive properties, such as NiO, CeO₂, and Al₂O₃, have yet to be synthesized in the form of hollow spheres. At the same time, since the chemical reactivities of different metallic element sources vary, any reaction model or process obtained from previous experiments on one synthetic system cannot be extended to others. Thus, establishing a general method using safe, inexpensive, and “user-friendly” reagents^[20] to synthesize various oxide hollow spheres is highly appealing. This would open up possibilities for extensive study of the physical and chemical properties of the most promising nanostructures and extend their applications.

Our group has recently developed a method for the preparation of Ga₂O₃ and GaN hollow spheres by using colloidal carbonaceous polysaccharide microspheres as templates.^[21,22] Herein, we report on an extension of this method to the synthesis of 12 other oxide hollow spheres, including main group metal oxide (Al₂O₃, SnO₂), transition metal oxide (ZrO₂, TiO₂, CoO, NiO, Cr₂O₃, Mn₃O₄), and rare earth oxide (La₂O₃, Y₂O₃, Lu₂O₃, CeO₂) hollow spheres by slightly modifying the procedures, and thus demonstrate a general protocol for obtaining metal oxide hollow spheres. Additionally, some cheese-like or macroporous films have also been prepared by templating the carbonaceous microspheres.

The surface-layer-adsorption and calcination (SLA-C) scheme for the fabrication of oxide hollow spheres by templating carbonaceous microspheres is illustrated in Figure 1.^[22] Carbonaceous microspheres, which serve as the templates, are first prepared from saccharide starting materials by dehydration under hydrothermal conditions.^[21] The surface of the spheres is hydrophilic, being functionalized with OH and C=O groups, and is similar in composition to polysaccharides according to previous IR, Raman, and EDS

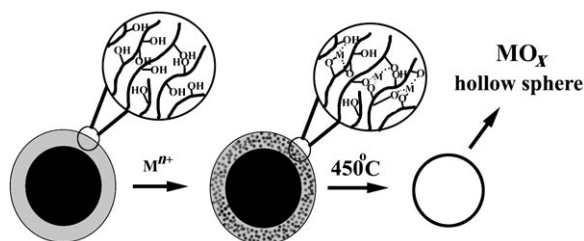


Figure 1. Schematic representation of the formation of metal oxide hollow spheres by using carbonaceous microspheres as templates.

studies.^[21] Upon dispersal of the carbonaceous microspheres in metal salt solutions, the functional groups in the surface layer are able to bind metal cations through coordination or electrostatic interactions. In the subsequent calcination process, the surface layers incorporating the cationic metal ions are densified and cross-linked to form oxide hollow spheres, replicas of the carbonaceous spheres but with reduced size (~40% of the original). This procedure offers some distinct advantages: 1) Cationic metal salts can be used as starting materials rather than alkoxides or metal oxide nanocrystals, which reduces preparation costs and saves experimental time since alkoxides are sensitive to humidity and monodisperse nanoparticles are not readily accessible. 2) Agglomeration is naturally avoided since the cations are absorbed into the surface layer to form a composite shell rather than forming a heterogeneous coating. 3) Appropriate selection of the transition-metal salts results in hollow spheres of the corresponding metal oxides, which makes the method a general one for the preparation of oxide hollow spheres. 4) Since the thickness of the functional “surface layer” is predetermined by the hydrothermal synthesis, the integrity and uniformity of the shells of the final products can be assured. 5) Additionally, since the functional groups on the surface of the microspheres are inherited from the saccharide, no surface modification or activation steps (as are typically required for polystyrene microspheres) are required. This reduces the number of processing steps and thus saves time. It is also demonstrated herein that this is a general method for obtaining oxide hollow spheres using the common cationic forms of main group metals (Al³⁺, Ga³⁺, Sn⁴⁺), transition metals (Mn²⁺, Ni²⁺, Cr³⁺, Co²⁺, Ti⁴⁺, Zr⁴⁺), and rare-earth metals (La³⁺, Y³⁺, Lu³⁺, Ce³⁺). The effects of changing the starting material from a metal salt to an alkoxide have been studied using TiO₂ as an example. Furthermore, this method has been extended to the preparation of cheese-like porous nanostructures and macroporous oxide films, as demonstrated using ZrO₂ and SnO₂.

Results and Discussion

Main group metal oxide hollow spheres: The synthesis of main group metal oxide hollow spheres was considered first to exemplify the sacrificial core method employing carbonaceous microspheres as templates. Oxides of Sn, Al, and Ga were studied, with particular emphasis on SnO₂. TEM images of SnO₂ samples prepared from aqueous solution are shown in Figure 2A,B, and may be compared with similar images of samples prepared from ethanolic solution shown in Figure 2C,D. All of the samples exhibited very similar hollow-sphere structures of uniform shape and size when the same carbonaceous spheres were used as templates. The size of the hollow spheres was about 40% of that of the original templates, confirming previous results.^[22] The shells of the hollow spheres in all of the samples were uniform, intact, and no more than 20 nm thick, which may be attributed to the similar characteristics of the surface layers of the

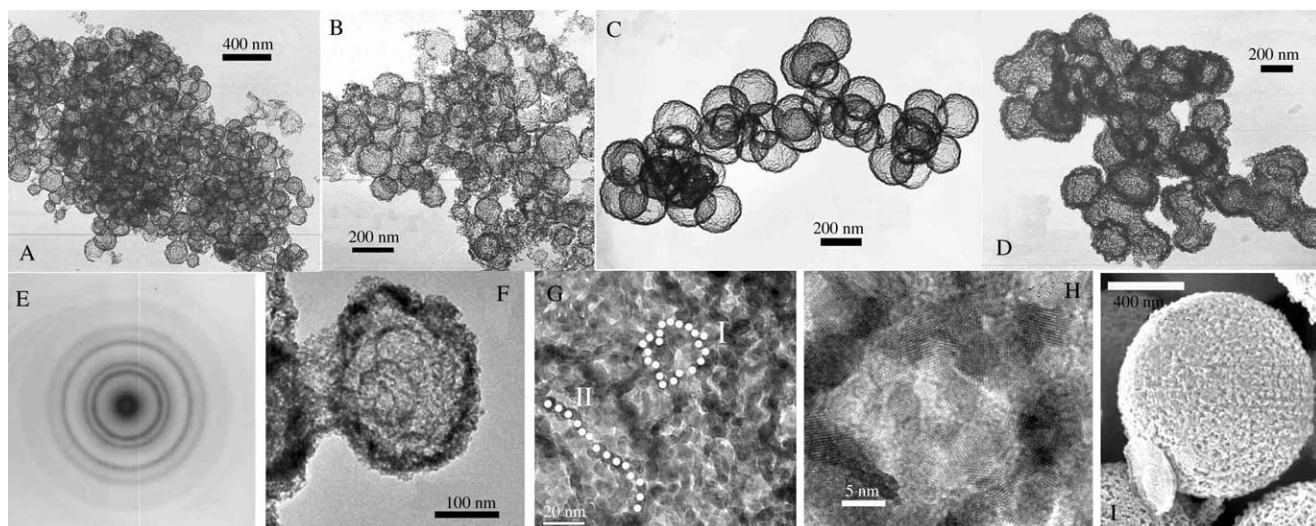


Figure 2. TEM and HRTEM images of SnO_2 hollow spheres: A) prepared from 0.05 M aqueous SnCl_4 solution; B) prepared from 0.2 M aqueous SnCl_4 solution; C) prepared from 0.05 M ethanolic SnCl_4 solution; D) prepared from 0.2 M ethanolic SnCl_4 solution; E) SAED pattern; F–H) HRTEM images of SnO_2 hollow spheres; I) high-resolution SEM image of template carbonaceous microspheres. (Areas I and II marked with white dots in G highlight the circle- and chain-like structures of the shell.)

carbonaceous microspheres.^[22] This implies that the carbonaceous template essentially determines the shape and structure of the final products. One inconspicuous difference is that the samples derived from aqueous solutions are associated with a small amount of nanoparticles that might be the products of hydrolysis during the Sn^{4+} adsorption process, whereas the samples from ethanolic solutions have quite smooth surfaces.

Concentration effects were studied in both the aqueous and ethanolic systems. No significant effects were observed when the same templates were used, except that when the concentrations of the respective solutions were increased from 0.05 M to 0.2 M, the fraction of small particles was slightly increased for the aqueous solution (Figure 2A,B), and the shell became somewhat thicker and coarser for the ethanol solution (Figure 2C,D). This implies that the functional layers of the carbonaceous spheres have quite strong interactions with the metal ions, and can be easily saturated with ions. This is further evidenced by the fact that the thickness of the SnO_2 hollow spheres varied little when the SnCl_4 concentration was increased beyond 0.2 M for the ethanolic system (see Supporting Information S1). All four samples were polycrystalline according to selected-area electron diffraction (SAED) patterns (Figure 2E) obtained from small nanocrystals less than 10 nm in size.

HRTEM images provide further insight into the structure of the SnO_2 hollow spheres (Figure 2F,G). A partly magnified image of individual hollow microspheres (Figure 2G) indicates that the nanocrystals that comprise the shell are all about 6 nm in size, and are in contact with one another to form circle- or chain-like structures (areas I and II in Figure 2G, where each white dot represents one nanocrystal). A further magnified image recorded on a “circle-like” structure confirms that the nanocrystals comprising the shell are single crystals with well-defined crystal lattices (Figure 2H).

These circle- or chain-like structures should correspond to the pore or pleat structures observed on the surfaces of the carbonaceous microspheres (Figure 2I). They provide further evidence that the oxide hollow spheres replicate the shells of the carbonaceous microspheres. Furthermore, the circle- or chain-like structures ensure that the nanoparticles are in contact with one another and are thus electrically conductive despite the macroporosity, which might be of value for the construction of electronic devices.

XRD patterns recorded from the samples indicated that the hollow spheres derived from the aqueous and ethanolic solutions were composed of crystals of essentially the same size (curves A and B in Figure 3, corresponding to 6.2 and

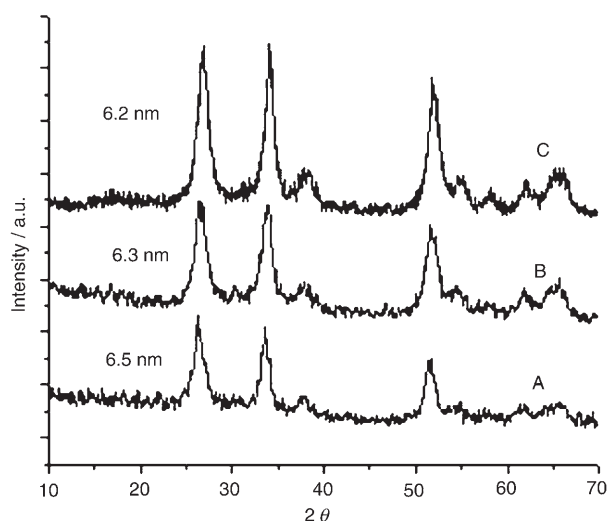


Figure 3. XRD patterns of SnO_2 prepared in different ways: A) nanoparticles precipitated from aqueous solution with ammonia; B) hollow spheres prepared from aqueous solution; C) hollow spheres prepared from ethanol solution.

6.3 nm, respectively, calculated using the Scherrer equation), and also essentially the same size as those prepared by neutralization with ammonia in aqueous solution (curve C in Figure 3, 6.5 nm). These results are in agreement with the TEM and HRTEM characterization, and further confirm that the nanocrystals comprising the shell are all single crystals.

This method was extended to the fabrication of Al_2O_3 hollow spheres (Figure 4A). Since $\text{Al}(\text{NO}_3)_3$ is not hydrolyzed like SnCl_4 , no fragments of Al_2O_3 were observed in

carbon cores formed by deeper carbonization of the precursor. These carbon spheres were oxidized when the temperature was further increased (to $\sim 431^\circ\text{C}$). A notable feature is that these template spheres retained their spherical profiles in spite of the decrease in size. This illustrates their advantageous use as templates for hollow spheres. If polystyrene spheres were used as templates, the composite spheres would melt at a temperature lower than 250°C if the shells could not provide sufficient mechanical stability by themselves. The carbonaceous saccharide spheres, on the other hand, only decrease in size, and always retain their spherical profile during calcination. It is for this reason that oxide hollow spheres may be prepared from metal salts by using the carbonaceous microspheres as templates.

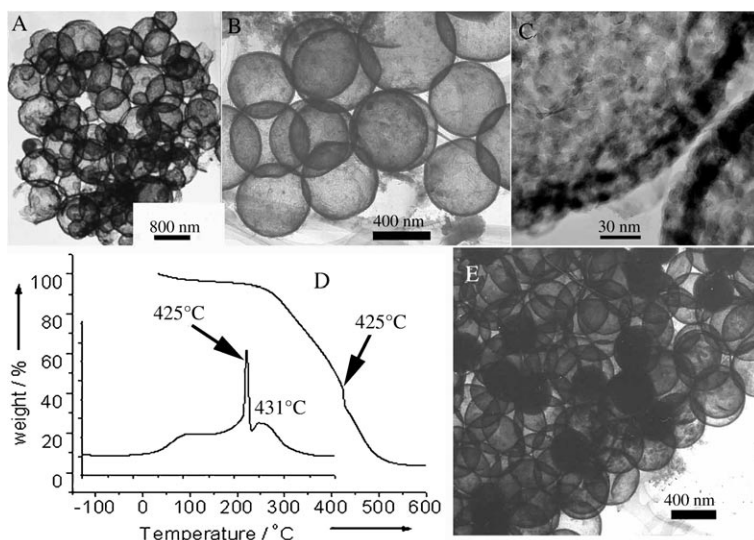


Figure 4. A) TEM image of Al_2O_3 hollow spheres; B) TEM and C) HRTEM images of Ga_2O_3 hollow spheres; D) TGA curve of carbonaceous saccharide spheres with absorbed Ga^{3+} ions (inset: the differential TGA curve); E) TEM image of Ga_2O_3 hollow spheres with residual small carbon spheres after insufficient calcination.

the sample. The size of the Al_2O_3 hollow spheres could be as large as 800 nm when larger template microspheres were used, which implies that the size of the oxide hollow spheres is predominantly determined by that of the template. Ga_2O_3 hollow spheres were also prepared in a similar way (Figure 4B,C). HRTEM characterization of these products showed the shell thickness to be about 20 nm. It did not change significantly even if the void size of the hollow spheres was enlarged or the type of oxide was varied.

In previous work, it was proposed that some deep-set carbonized spheres might exist after the first oxidation. This has now been evidenced by analysis of thermogravimetric analysis (TGA)/differential thermal analysis (DTA) curves (Figure 4D) and TEM characterization (Figure 4E). The TGA curve shows weight loss to occur in three stages: below 425°C , at 425°C , and above 425°C . These stages correspond to the three steps of the formation of oxide hollow spheres during calcination: densification, surface oxidation, and oxidation of residual deep-set carbonized spheres. When the calcination time was insufficient, some carbon spheres far smaller than the templates (~ 200 nm rather than ~ 800 nm) were observed. These should be the residual

Transition-metal and rare-earth oxide hollow spheres: Since our method uses metal salts as starting materials, it is advantageous for the synthesis of transition metal and rare earth oxide hollow spheres. Typical images of the oxide hollow spheres obtained are shown in Figure 5. Most of the hollow spheres are uniform and intact. The size of the hollow spheres could be made as large as 800 nm (Figure 5B) or as small as 60 nm (Figure 5F) by using template spheres of various

sizes. The results further evidenced that the sizes and structures of the hollow spheres are predetermined by the sizes and functional layer structures of the template carbonaceous spheres, and are less dependent on the nature of the metal ions. The crystal structures of the hollow spheres were carefully characterized by analysis of their SAED and XRD patterns (see Supporting Information, S2 and S3). The results indicated that they were cubic NiO (space group $Fm\bar{3}m$, 225), cubic CoO (space group $Fm\bar{3}m$, 225), tetragonal Mn_3O_4 (space group $I41/amd$, 141), and rhombohedral Cr_2O_3 (space group $R\bar{3}c$, 167). All of the hollow spheres were polycrystalline according to analysis of their SAED patterns.

Detailed studies on the synthesis of rare earth oxide hollow spheres, such as those of La_2O_3 and Y_2O_3 , and their optical properties have been reported previously.^[23] Some images are shown in the Supporting Information (S4). Herein, we report two new types of rare-earth oxide hollow spheres, namely those of Lu_2O_3 and CeO_2 ; their TEM images are shown in Figure 5E,F. These hollow spheres offer clear advantages over their solid counterparts because of their low density, porous structure, and encapsulation ability.

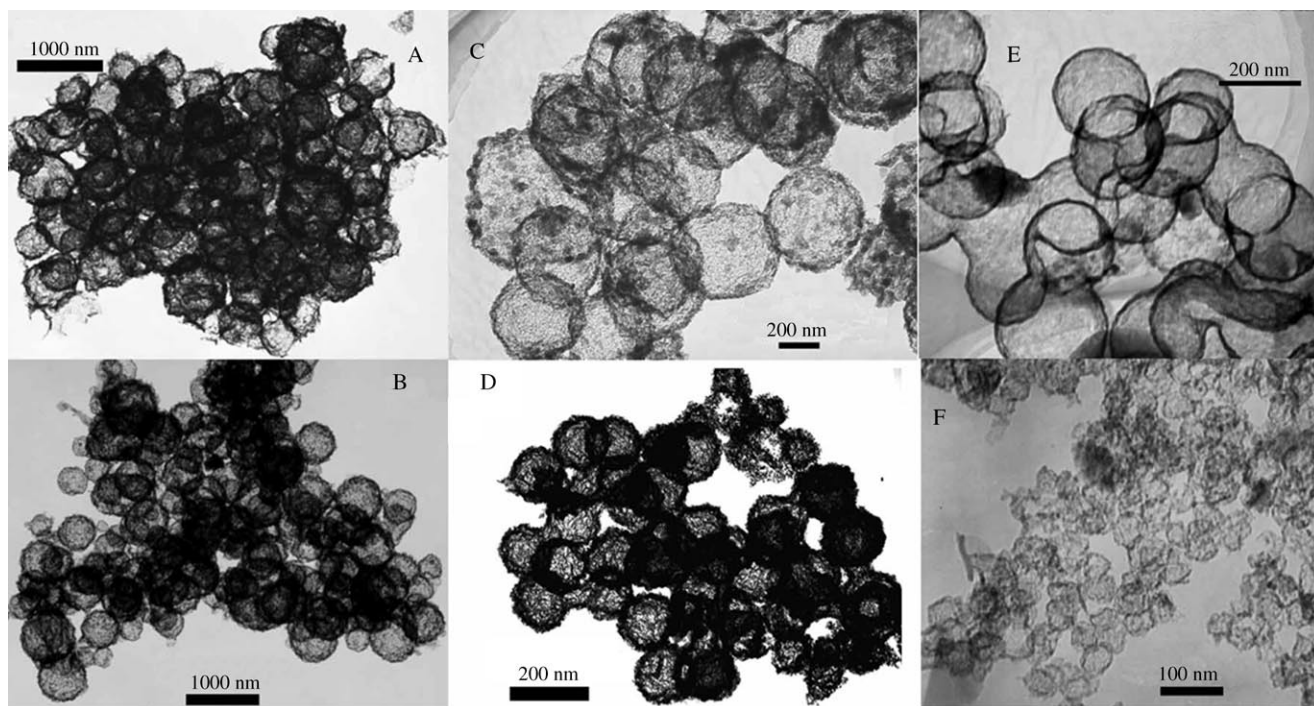


Figure 5. TEM images of transition-metal and rare-earth oxide hollow spheres: A) CoO; B) Mn₃O₄; C) NiO; D) Cr₂O₃; E) CeO₂; F) Lu₂O₃.

Furthermore, since most transition metals and rare earth elements have rich chemistries based on d- and f-orbital electrons and variable valence states, these hollow spheres have great potential for applications in the area of catalysis or as catalyst supports.

Comparison of effects of starting materials (synthesis of TiO₂ hollow spheres): Different starting materials, that is, metal salts or metal alkoxides, were found to affect the structures of the final products. This was evidenced in the synthesis of TiO₂ hollow spheres. Figure 6A,B show TEM images of TiO₂ hollow spheres prepared by templating carbonaceous microspheres (~800 nm) using TiCl₄ as starting material in ethanolic solution. It can be seen that the voids are about 350 nm in size and that the shells are about 20 nm thick and are composed of small nanocrystals (<10 nm). This structure is very similar to those of other oxide hollow spheres, such as the Ga₂O₃ product, described above. However, when the starting material was changed to tetrabutyltitanate, the shell thickness increased to more than 100 nm (Figure 6C,D) and the void size increased to about 800 nm, essentially the same as that of the templates.

The differences in the structures of the products stemmed from different formation mechanisms. As the Ti⁴⁺ ions were absorbed in the functional layer of the carbonaceous microspheres, they were dilutely dispersed in the shell, and thus offered insufficient mechanical stability prior to densification and cross-linking to form a continual oxide shell. The densification process during calcination led to a decrease in diameter to 40% of the original. However, the mechanism changed when tetrabutyltitanate was used as starting materi-

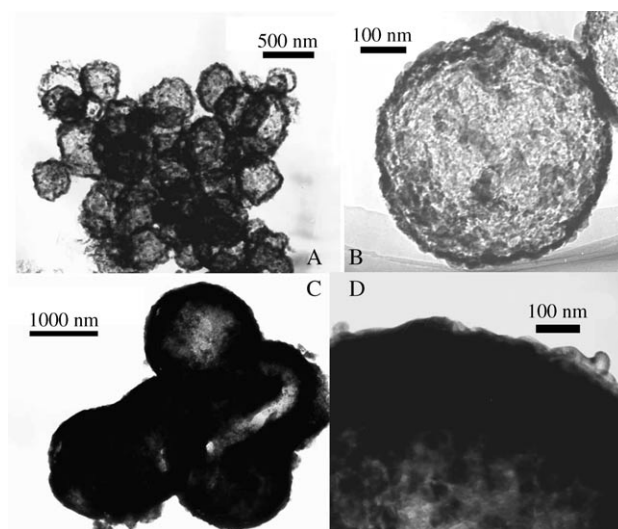


Figure 6. TEM images of TiO₂ hollow spheres: A, B) prepared by using Ti⁴⁺ as starting material; C, D) prepared by using tetrabutyltitanate as starting material.

al. No reaction took place in an ethanolic suspension of tetrabutyltitanate and carbonaceous microspheres until a mixture of water and ethanol was introduced, as in the case of the formation of WO₃ hollow spheres.^[24] The polysaccharide-like hydrophilic surface of the spheres, bearing hydroxyl groups (-OH), favored the hydrolysis of tetrabutyltitanate. Thus, a shell of TiO₂ precursor formed on the surface. The shell thickness increased as the hydrolysis proceeded. The core-shell structures thus formed showed some distinctive

differences to those prepared by ion absorption into surface layers: 1) The oxide precursor coating layer was continual and had sufficient mechanical stability to maintain the hollow spherical structure when the template carbonaceous cores were removed, so the as-formed void size was nearly the same as that of the template spheres, rather than ~40% in the densification and cross-linking mechanism. 2) The thickness of the oxide shell could be 100 nm or more, and could be manipulated by adjusting the experimental parameters. However, in the surface layer ion absorption method, the shell thickness was predetermined by the thickness of the functional layer of the template, and could not be readily increased. These results suggest that carbonaceous microspheres can also serve as versatile templates for thick-shell oxide hollow spheres. 3) The formation of agglomerations is relatively easier when solid-state precursor coating rather than surface ion absorption is used to form precursive composite spheres.

ZrO₂ hollow spheres, cheese-like structures, and SnO₂ macroporous thin films: Uniform and intact ZrO₂ hollow spheres prepared by the surface layer ion absorption method are shown in Figure 7A,B. When some residual Zr⁴⁺

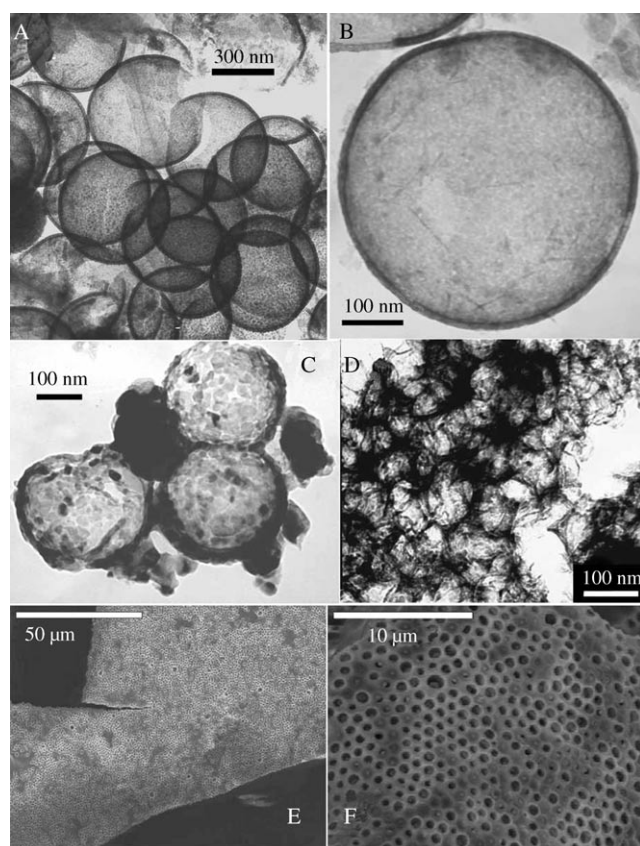


Figure 7. A, B) ZrO₂ hollow spheres prepared by the surface layer ion absorption method; C) ZrO₂ hollow spheres with nanoparticles bridging two or more hollow spheres; D) cheese-like structure of ZrO₂ obtained when ZrOCl₂ solution was deliberately added; E, F) general and magnified images of SnO₂ porous films prepared by templating carbonaceous polysaccharide spheres.

-containing solution from the rinsing process was retained between several ion-absorbed carbonaceous spheres, these could be converted into nanoparticles by the bridging of two or more hollow spheres (Figure 7C). This suggested that the deliberate addition of some Zr source could lead to macroporous nanostructures. Figure 7D shows the macroporous cheese-like structure of ZrO₂ obtained when a 0.01 M ZrOCl₂ solution was added and neutralized with ammonia. The by-product NH₄Cl would be volatilized and the carbonaceous template would be oxidized under the calcination conditions, and thereby cheese-like ZrO₂ nanostructures with spherical voids could be formed.

The above method could easily be extended to the synthesis of SnO₂ macroporous thin films. In this case, the concentration of SnCl₄ deliberately added was increased to 0.1 M. After neutralization with ammonia and calcination to remove the spherical templates, macroporous films were formed (Figure 7E,F). These macroporous materials have potential uses in the fabrication of sensors, filters, or other functional devices.^[1,25]

Accessible and inaccessible hollow spheres: As demonstrated above, our method could be used to fabricate many kinds of metal oxide hollow spheres. However, results have also indicated that certain oxide hollow spheres cannot be prepared in this way. For instance, attempted syntheses of PbO and Bi₂O₃ hollow spheres by templating carbonaceous polysaccharide spheres with Pb(OAc)₂·3H₂O and BiCl₃ solutions were unsuccessful. This might relate to the low melting points of the elements (Pb: 327.4°C, Bi: 271.4°C) or increased volatilization because of locally reductive atmospheres formed in the presence of large amounts of carbonaceous microspheres. On the other hand, according to experimental results, the metal source, especially the charge state of metal ions, is critical for absorption and consequent formation of the hollow spheres. For instance, WCl₆, but not Na₂WO₄, can be used as a starting material for the synthesis of WO₃ hollow spheres because the surface of the carbonaceous spheres is negatively charged.^[24] Attempted use of negatively charged vanadate or borate to prepare the corresponding oxide hollow spheres met with failure, further demonstrating that only positively charged metal ions may be used in this method.

Gas sensitivity of SnO₂ hollow spheres: The porous structures and consequent lower densities and larger specific surface areas of the hollow spheres make them promising for applications in fields where surface-related properties are dominant, such as catalysis or gas sensitivity. In previous work, we have demonstrated the gas sensitivity of WO₃ hollow spheres^[24] and the photoluminescence properties of rare earth compound hollow spheres.^[23] In the present work, we have identified a “quick-recovery” property of SnO₂ hollow spheres when using them in a gas sensor.

In a previous study, the gas sensitivity of WO₃ hollow spheres was compared with that of some belt-like powders.^[24] However, these two samples were prepared from dif-

ferent solutions by way of various methods and thus had different crystal sizes, and so the structural effects (i.e., hollow spheres or particles) could not be fully delineated since gas sensitivity is extremely dependent on surface properties and crystal size. In the present study, SnO₂ hollow spheres, composed of nanoparticles (6.2–6.3 nm), have been compared with nanopowders of nearly the same size (6.5 nm) prepared by ammonia precipitation from aqueous solutions. Two types of hollow spheres with nearly the same crystal size, obtained from aqueous and ethanolic solutions, respectively, were used to construct sensors, and these were compared to provide insight into the effects of experimental procedure or final structure. The crystal size was estimated on the basis of Scherrer equation calculation on the XRD patterns (Figure 3).

The response time of a sensor is defined as the time required for a change in sample conductance to reach 90% of the equilibrium value following the injection of a test gas. Similarly, the recovery time is defined as the time required for the sample to show a 90% reversal of this conductance change as the test gas is released. According to gas-sensitivity measurement results (Figure 8A), all three of our sensors showed response times to ethanol of as short as 10 s, and the sensitivities of the three sensors were all close to 10 at a concentration as low as 10 ppm. Thus, we can easily detect concentrations well below the limit imposed for a breath analyzer (~200 ppm).^[26] This result implies that the sensitivity of the SnO₂ sensors is mainly determined by crystal size, and not by the type of precursor solution or the structure (hollow spheres or particles) of the sample.

However, in contrast to the reaction curves, which remained essentially the same, the recovery curves varied significantly. Sensors prepared with the hollow spheres exhibited excellent “quick-recovery” properties, while those made from nanopowders recovered quite slowly. Response curves of the three sensors at around 100 ppm have been magnified to highlight the differences between those obtained from the hollow spheres and that obtained from nanoparticles (Figure 8B). It can clearly be seen that the recovery time of the nanopowder sensor is as long as 100 s, whereas the recovery times of the two hollow-sphere sensors are about 14 s. This also implies that the much reduced recovery time is induced by the hollow-sphere structure, and is not related to whether the synthetic system is based on aqueous or ethanolic solutions. On increasing the concentration of working gas (10 ppm→500 ppm) and prolonging the working time (100 s→140 s), the recovery time required for the two hollow-sphere sensors increased only marginally (by 4 s). This gives evidence of their working stability. It is worthy of note that this recovery time of the hollow-sphere sensors is even shorter than that of a thin-film sensor epitaxially grown on sapphire (30 s).^[27] The “quick-recovery” property is of particular interest in cases where the concentration of the gas to be detected is subject to fluctuation, or the sensor is used almost continually with very short “rest” time.

The “quick-recovery” property is appealing since sensors tend to lack the ability to respond to a low concentration of

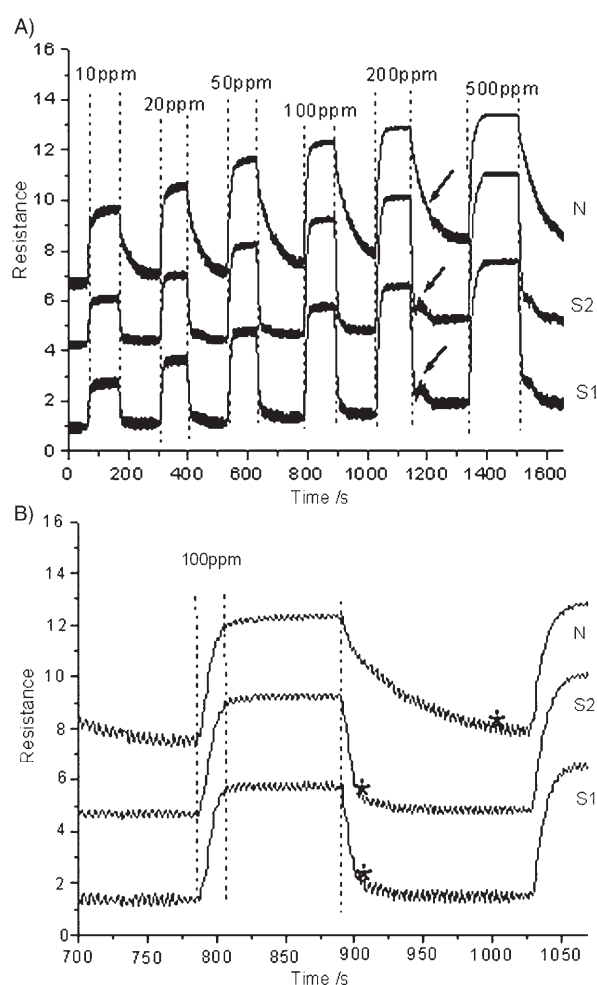


Figure 8. A) Typical response curves on switching between increasing concentrations (10–500 ppm) of ethanol and ambient air. B) Partly magnified response curves at a concentration of 100 ppm to exhibit the “quick-recovery” as marked with asterisks. (N: nanoparticles from aqueous solution; S1: hollow spheres from ethanolic solution; S2: hollow spheres from aqueous solution).

the test gas during the process of recovering. A deliberate fluctuation in the ethanol concentration highlighted this point. During the measurement at a level of about 200 ppm, when the recovery time was 15 s, the ethanol concentration was suddenly increased somewhat. Both the hollow-sphere sensors responded quickly (as marked with arrows in Figure 8A), while the response of the sensor made of nanoparticles continued to follow the same downward trend.

As a typical n-type semiconductor, SnO₂-based gas sensors have become the predominant solid-state devices for gas alarms used on domestic, commercial, and industrial premises since 1962.^[27] Decreasing the response and recovery times is one of the three basic problems for gas-sensor design.^[28,29] The present study thus has strong practical application potential.

The much reduced recovery time should be closely related to the macroporous structure of the hollow spheres. The recovery of a sensor can be considered to relate mainly to two

steps: dissociation of test molecules from the sensor and their diffusion out of the film. The much reduced recovery time should be mainly related to the shortened diffusion time caused by the macroporous structure. When the hollow spheres were coated as a thick film on the surface of ceramic tubes, a large number of voids several hundreds of nanometers in size remained among/inside the accumulation of hollow spheres. The circle- or chain-like structures of the hollow spheres ensured electronic conductivity of the gas sensor. The loose and porous structure is clearly far more favorable for the diffusion of gas molecules than that of a sensor constructed from a nanopowder. In the latter case, a relatively compact film with low void density and far smaller void size would be formed. The void size would be less than 10 nm, one or two orders of magnitude smaller than that of a hollow-sphere sensor.

Thus, the structure and morphology of the particles can be correlated with the sensor performance. When gas-phase ethanol molecules diffuse and reach the surface of the SnO₂ film, the resistance of the SnO₂ sensors increases sharply to give a measurable response because of a surface chemical reaction. Previous studies on SnO₂-based gas sensors have indicated that surface states, grain boundaries, and grain size are important parameters for the response to gas molecules in SnO₂ gas sensors.^[27–29] These factors are similar for the three sensors, so their reaction performances are similar. However, the recovery time is mainly determined by the diffusion process, hence a difference emerged between the hollow-sphere sensors and that constructed from a nanopowder. As the working time is extended, the test molecules penetrate deeper into the thick sensor films and cause chemical reactions therein. In the case of the hollow-sphere sensors, the film is macroporous with an actual thickness of less than 20 nm, that is, that of the hollow-sphere shell. The voids in and among the hollow spheres provide an ideal pathway through which the gaseous ethanol molecules can diffuse out and away after their release. Thus, the hollow-sphere sensors can easily regain their original resistance in a very short time. In the case of the nanopowder sensor, however, the thick, compact SnO₂ film with its smaller void size impedes diffusion of the ethanol molecules, and hence the device is unable to recover in a short time.

Conclusion

A general method has been developed for the fabrication of metal oxide hollow spheres by using carbonaceous polysaccharide microspheres as templates. Since metal salts are used as starting materials and functional layers are naturally formed in template preparation, the range of accessible metal oxide hollow spheres is increased and the fabrication procedures are shortened. Macroporous films or cheese-like nanostructures of oxides can also be prepared by slightly modified procedures. Other types of hollow spheres of metal compounds, such as nitrides, carbides, monosulfide oxides or oxyhalides, might be derived from the as-formed

oxide hollow spheres or precursive ion-absorbed composite spheres.^[22,23,30,31] Thus, the structure, size, and composition of hollow or composite particles may be varied in a controllable way to tailor their optical, electrical, thermal, mechanical, electro-optical, magnetic, and catalytic properties over a broad range. A preliminary study on the gas sensitivity of SnO₂ hollow spheres has revealed a considerably reduced sensor “recovery time”, which exemplifies the distinct properties imparted by the hollow structure.

Experimental Section

Materials: All reagents were of analytical grade, purchased from the Beijing Chemical Reagent Factory, and were used as received without further purification.

Synthesis of template carbonaceous microspheres: In a typical procedure, glucose (~4–8 g) was dissolved in deionized water (40 mL) to form a clear solution. The solution was then sealed in a 40 mL autoclave with a Teflon seal and maintained at 160–180 °C for 4–20 h. Black or dark-purple puce products were obtained after centrifugation at 5000 rpm for 20 min. A rinsing process involving five cycles of centrifugation/washing/redispersion was performed with water or ethanol, respectively. The final samples were obtained after oven-drying at 80 °C for more than 4 h.

It was found that changing the starting material from glucose to sucrose or another soluble saccharide (e.g., corn starch) also led to fairly monodisperse microspheres under similar conditions.

Synthesis of metal oxide hollow spheres: In a typical procedure, the requisite metal salt was first dissolved in 10–40 mL of the appropriate solvent so as to form a solution of concentration 0.05–0.5 M. For the salts that are not hydrolyzed in water (LaCl₃, YCl₃, LuCl₃, Ce(NO₃)₃, Al(NO₃)₃, GaCl₃, CoCl₂, NiSO₄, Cr(NO₃)₃, Mn(NO₃)₂, ZrOCl₂), deionized water was used as solvent. In the case of the hydrolyzable TiCl₄, ethanol was used. In the case of SnCl₄, both media were used for comparison.

Oven-dried carbonaceous microspheres (100 mg) were evenly dispersed in the aforementioned solutions with the assistance of ultrasonication. The ultrasonication was continued for 40–80 min to ensure sufficient diffusion of the metal ions into the surface layer. A rinsing process involving 3–5 cycles of centrifugation/washing/redispersion was performed with either water or ethanol, according to the solvent used initially. The black or puce samples obtained were oven-dried at 80 °C for 4 h and used as precursors of the hollow spheres.

The samples obtained after ion absorption as described above were transferred to alumina crucibles, and these were placed in a muffle furnace. Calcination was carried out in air. In typical procedures, the calcination parameters were set as 450 °C for 2 h or 500 °C for 1 h. The furnace was then left to cool to room temperature. As-formed products were accumulated at the bottom of the crucibles.

Template synthesis of thick-shell TiO₂ hollow spheres: Thick-shell TiO₂ hollow spheres were prepared using tetrabutyltitanate as starting material. Tetrabutyltitanate (5 mL) was dissolved in ethanol (35 mL) to form a clear solution. Carbonaceous spheres (~100 mg) were then dispersed in the freshly prepared solution with the aid of ultrasonication for 5 min. A 1:5 (v/v) mixture of water and ethanol was added dropwise to the suspension of carbonaceous spheres with vigorous magnetic stirring over a period of approximately 15 min. Thereafter, the suspension was stirred for a further 1 h before centrifugation and washing with ethanol. After five cycles of centrifugation/washing/redispersion with ethanol, the powder obtained was oven-dried and calcined according to the procedure described above.

Synthesis of cheese-like ZrO₂ nanostructures and macroporous SnO₂ films: Oven-dried carbonaceous microspheres (100 mg) were evenly dispersed in 0.1 M aqueous ZrOCl₂ solution with the aid of ultrasonication. Ultrasonication was continued for a further 1 h to ensure sufficient diffusion of metal ions into the surface layer. The suspension was then centri-

fused at 5000 rpm for 20 min. The supernatant clear solution was removed and 0.01 M aqueous $ZrOCl_2$ solution (1 mL) was added to the precipitate. A very thick suspension was formed after ultrasonication for 10 min. This suspension was then neutralized with ammonia under sonication. As in the previous preparations, it was transferred to crucibles and calcined at 450 °C for 2 h. The samples were left to cool naturally to room temperature to produce the final products.

The procedure for preparing SnO_2 macroporous films was very similar to that for the ZrO_2 cheese-like structure. Carbonaceous spheres (~100 mg) were dispersed and sonicated in 0.1 M aqueous $SnCl_4$ solution for more than 40 min. Thus, 0.1 M aqueous $SnCl_4$ solution (1 mL) was added to the precipitate obtained after centrifugation and removal of the supernatant solution. Aqueous ammonia aqueous solution was added to adjust the pH value to 9, also under sonication. The slurry-like mixture was then further sonicated for 10 min before spreading it on Si wafers. The wafers were placed in crucibles and calcined in a muffle furnace at 450 °C for 2 h.

Characterization of the samples: Powder X-ray diffraction (XRD) analysis was performed on a Bruker D8 Advance X-ray diffractometer using monochromated $Cu_{K\alpha}$ radiation ($\lambda = 1.5418 \text{ \AA}$). The size and morphology of the oxide hollow spheres were measured using a Philips 1200 transmission electron microscope (TEM) operated at 120 KV and a JEOL JEM-2010F high-resolution transmission electron microscope (HRTEM) operated at 200 KV.

Gas-sensitivity measurements were performed using ethanol as a probe molecule in a commercial HW-30 gas-sensing measurement system, which comprised a static vessel with a movable cover, and a resistance data collection system. The gas sensors were fabricated using thin films prepared from suspensions of SnO_2 hollow spheres or nanoparticles. As-formed hollow spheres and nanoparticles were dispersed in tetraethyl orthosilicate and then slightly ground to form a slurry. No conductive binder was added. A schematic diagram of a typical gas sensor is shown in the Supporting Information (S5), using that prepared with SnO_2 hollow spheres as an example. Ceramic Al_2O_3 tubes were used as mechanical substrates for gas-sensing SnO_2 films composed of hollow microspheres. Circular Au electrodes were positioned at both ends of the tubes. Four Pt leads extended from the Au electrodes to connect them to external signal detectors. A slurry of SnO_2 and tetraethyl orthosilicate (TEOS) was coated onto the external surface of the ceramic tube to connect the two Au electrodes. After coating, the system was calcined at 450 °C for 2 h to densify the film. Measurements were carried out at a temperature of about 250 °C. The test gas was introduced into the testing chamber by injection.

Acknowledgements

We sincerely thank Prof. Joseph F. Chiang, Chemistry Department, State University of New York (SUNY) at Oneonta, USA, for helpful discussions. This work was supported by the NSFC (90406003, 20401010, 50372030, 20025102, 20131030), the Foundation for the Author of National Excellent Doctoral Dissertation of the P. R. China, and the State Key Project of Fundamental Research into Nanomaterials and Nanostructures (2003CB716901).

- [1] J. K. Cochran, *Curr. Opin. Solid State Mater. Sci.* **1998**, *3*, 474–479.
[2] Y. N. Xia, B. Gates, Y. D. Yin, Y. Lu, *Adv. Mater.* **2000**, *12*, 693–713, and reference therein.

- [3] F. Caruso, *Top. Curr. Chem.* **2003**, *227*, 145–168, and references therein.
[4] P. Jiang, J. F. Bertone, V. L. Colvin, *Science* **2001**, *291*, 453–457.
[5] M. Iida, T. Sasaki, M. Watanabe, *Chem. Mater.* **1998**, *10*, 3780–3782.
[6] T. Nakashima, N. Kimizuka, *J. Am. Chem. Soc.* **2003**, *125*, 6386–6387.
[7] Q. Peng, Y. J. Dong, Y. D. Li, *Angew. Chem.* **2003**, *115*, 3135–3138; *Angew. Chem. Int. Ed.* **2003**, *42*, 3027–3030.
[8] M. Yang, J. J. Zhu, *J. Cryst. Growth* **2003**, *256*, 134–138.
[9] H. G. Yang, H. C. Zeng, *J. Phys. Chem. B* **2004**, *108*, 3492–3495.
[10] Y. D. Yin, R. M. Rioux, C. K. Erdonmez, S. Hughes, G. A. Somorjai, A. P. Alivisatos, *Science* **2004**, *304*, 711–714.
[11] L. M. Liz-Marzán, M. Giersig, P. Mulvaney, *Langmuir* **1996**, *12*, 4329–4335.
[12] R. T. Tom, A. S. Nair, N. Singh, M. Aslam, C. L. Nagendra, R. Philip, K. Vijayamohan, T. Pradeep, *Langmuir* **2003**, *19*, 3439–3445.
[13] I. Pastoriza-Santos, D. S. Koktysh, A. A. Mamedov, M. Giersig, N. A. Kotov, L. M. Liz-Marzán, *Langmuir* **2000**, *16*, 2731–2735.
[14] K. P. Velikov, A. van Blaaderen, *Langmuir* **2001**, *17*, 4779–4786.
[15] a) Z. Y. Zhong, Y. D. Yin, B. Gates, Y. N. Xia, *Adv. Mater.* **2000**, *12*, 206–209; b) Y. Lu, Y. D. Yin, Y. N. Xia, *Adv. Mater.* **2001**, *13*, 271–274.
[16] a) F. Caruso, *Chem. Eur. J.* **2000**, *6*, 413–419; b) F. Caruso, M. Spasova, A. Susha, M. Giersig, R. A. Caruso, *Chem. Mater.* **2001**, *13*, 109–116.
[17] Z. Z. Yang, Z. W. Niu, Y. F. Lu, Z. B. Hu, C. C. Han, *Angew. Chem.* **2003**, *115*, 1987–1989; *Angew. Chem. Int. Ed.* **2003**, *42*, 1943–1945.
[18] L. Z. Wang, T. Sasaki, Y. Ebina, K. Kurashima, M. Watanabe, *Chem. Mater.* **2002**, *14*, 4827–4832.
[19] D. B. Wang, C. X. Song, Z. S. Hu, X. Fu, *J. Phys. Chem. B* **2005**, *109*, 1125–1129.
[20] X. G. Peng, *Chem. Eur. J.* **2002**, *8*, 335–339.
[21] X. M. Sun, Y. D. Li, *Angew. Chem.* **2004**, *116*, 607–611; *Angew. Chem. Int. Ed.* **2004**, *43*, 597–601.
[22] X. M. Sun, Y. D. Li, *Angew. Chem.* **2004**, *116*, 3915–3919; *Angew. Chem. Int. Ed.* **2004**, *43*, 3827–3831.
[23] H. Y. Wang, R. J. Wang, X. M. Sun, R. X. Yan, Y. D. Li, *Mater. Res. Bull.* **2005**, *40*, 911–919.
[24] X. L. Li, T. J. Lou, X. M. Sun, Y. D. Li, *Inorg. Chem.* **2004**, *43*, 5442–5449.
[25] See, for example: a) Y. N. Xia, Y. D. Yin, Y. Lu, J. McLellan, *Adv. Funct. Mater.* **2003**, *13*, 1–12; b) O. D. Velev, A. M. Lenhoff, *Curr. Opin. Colloid Interface Sci.* **2000**, *5*, 56–63; c) C. F. Blanford, H. W. Yan, R. C. Schroden, M. Al-Daous, A. Stein, *Adv. Mater.* **2001**, *13*, 401–407; d) R. A. Caruso, *Top. Curr. Chem.* **2003**, *226*, 91–118.
[26] J. F. Liu, X. Wang, Q. Peng, Y. D. Li, *Adv. Mater.* **2005**, *17*, 764–767.
[27] D. S. Lee, G. H. Rue, G. S. Huh, S. D. Choi, D. D. Lee, *Sens. Actuators B* **2001**, *77*, 90–94.
[28] W. Gopel, K. D. Schierbaum, *Sens. Actuators B* **1995**, *26–27*, 1–12.
[29] G. S. Korotchenkov, S. V. Dmitriev, V. I. Brynzari, *Sens. Actuators B* **1999**, *54*, 202–209.
[30] Y. D. Li, Y. Huang, T. Bai, L. Q. Li, *Inorg. Chem.* **2000**, *39*, 3418–3420.
[31] X. L. Li, Y. D. Li, *Chem. Eur. J.* **2004**, *10*, 433–439.

Received: June 8, 2005

Revised: November 15, 2005

Published online: December 23, 2005